IXPE-SOC-DOC-008
National Aeronautics and Space Administration
Revision A
EFFECTIVE DATE: 2022-07-22

George C. Marshall Space Flight Center
Marshall Space Flight Center, Alabama 35812

ST-12

IMAGING X-RAY POLARIMETRY EXPLORER (IXPE)
SCIENCE OPERATIONS CENTER (SOC)

User Guide — Instrument

IXPE Science Operations Center
User Guide to the Instrument

Signatures

APPROVED BY

KURTIS DIETZ Digitally signed by KURTIS DIETZ
Date: 2022.07.19 09:31:02 -05'00'

Kurt Dietz /ES63
SOC Software Lead

ALLYN TENNANT Digitally signed by ALLYN TENNANT
Date: 2022.07.19 13:26:04 -04'00'

Allyn F. Tennant /ST12
SOC Lead

STEPHEN O'DELL Digitally signed by STEPHEN O'DELL
Date: 2022.07.18 15:46:59 -05'00'

Stephen L. O'Dell /ST12
Project Scientist

BRIAN RAMSEY Digitally signed by BRIAN RAMSEY
Date: 2022.07.18 16:49:51 -05'00'

Brian D. Ramsey /ST12
Deputy Principal Investigator

Revision Log

Date	Rev	Notes
2021-11-08	Baseline	Baseline version
2022-07-15	A	Formatting changes to improve consistency with other IXPE User Guides

TABLE OF CONTENTS

1. INSTRUMENT OVERVIEW 5
   1.1. DETECTOR UNITS 5
   1.1.1. DESIGN 5
   1.1.2. DU PERFORMANCE 7
   1.1.2.1. QUANTUM EFFICIENCY 7
   1.1.2.2. ENERGY RESOLUTION 8
   1.1.2.3. SPATIAL RESOLUTION 8
   1.1.2.4. MODULATION FACTOR 9
   1.1.2.5. SPURIOUS MODULATION 10
   1.1.2.6. RATE-DEPENDENT GAIN VARIATIONS 11
   1.1.2.7. LONG-TERM FILL-GAS-PRESSURE VARIATION 11
   1.1.2.8. BACKGROUND 12
   1.1.3. FILTER/CALIBRATION WHEEL 12
   1.2. DETECTORS SERVICE UNIT (DSU) 13
2. INSTRUMENT OPERATION 14
   2.1. MODES OF OPERATION 14
   2.2. DEAD TIME / RATE CAPABILITY 15
   2.3. HOT PIXEL MASKING 16
   2.4. TIMING 16
3. REFERENCES 18

1 INSTRUMENT OVERVIEW

The IXPE instrument is an Italian contribution funded by the Italian Space Agency (ASI) through the Istituto di Astrofisica e Planetologia Spaziali (IAPS) and the Istituto Nazionale di Fisica Nucleare (INFN). It comprises three flight Detector Units (DU) and a single Detectors Service Unit (DSU). The DUs each contain a gas pixel detector, which is essentially the heart of the instrument. Inside the GPD is a gas cell, holding the detection medium, and a custom ASIC to read the signals out. The DU also contains the back-end electronics which process the data and a filter and calibration wheel assembly (FCW). The DSU provides the three DUs with the required power, controls the FCW, and formats the scientific data and forwards it to the spacecraft computer for storage and eventual transmission to the ground.

1.1 Detector Units

1.1.1 Design

The heart of the IXPE payload are the detector units (DUs). Located at the focus of each MMA these provide position sensitivity, energy determination, timing information and, most importantly, polarization sensitivity. Inside each DU is a Gas Pixel Detector[1,2,3] (GPD) which images the photoelectron tracks produced by x-rays absorbed in the special fill gas (Dimethyl Ether - DME). The initial emission direction of the photoelectron contains the necessary information to determine the polarization of the source, while the initial interaction point and the total charge in the track provide the location and energy of the absorbed x ray, respectively.

Figure 1 shows a schematic of the GPD. An x ray enters through a beryllium window and interacts in the DME fill gas. The resulting photoelectron leaves a trail of ionization, and this photoelectron track drifts through a Gas Electron Multiplier (GEM), to provide charge gain, and onto a pixel anode readout. Table 1 gives the relevant performance parameters.

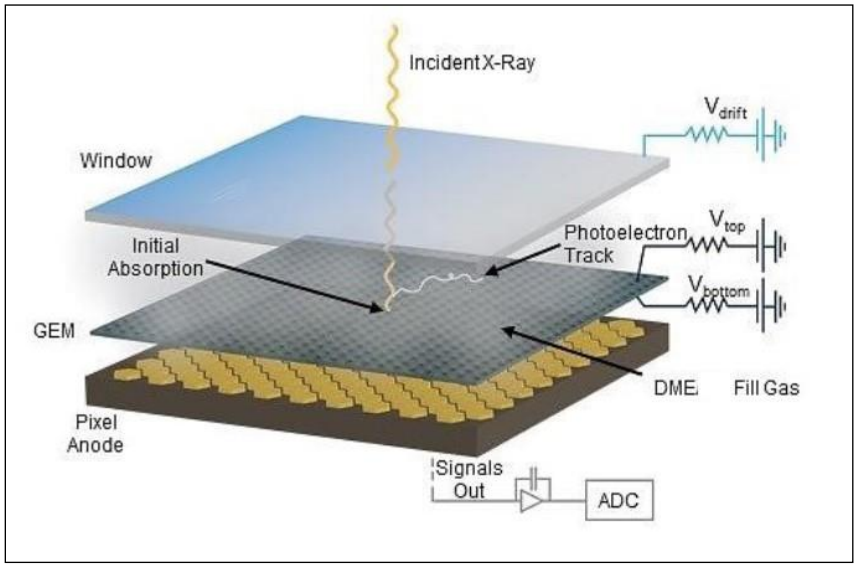

Figure 1: Schematic of the Gas Pixel Detector (GPD)

Table 1: Performance parameters of an IXPE Detector Unit (DU)

Parameter	Value
Sensitive area	15 mm × 15 mm (13 x 13 arcmin)
ASIC readout pitch	50 µm
Fill gas and asymptotic pressure	DME @ ~ 650 mbar
Detector window	50-µm thick beryllium
Absorption and drift region depth	10 mm
Spatial resolution (FWHM)	≤ 123 µm (6.4 arcsec) @ 2 keV
Energy resolution (FWHM)	0.57 keV @ 2 keV ($\propto \sqrt{E}$)
Useful energy range	2 - 8 keV

An expanded view of a detector unit is shown in Figure 2 (left). As well as the GPD, the unit houses all of the back-end electronics to process each event, as well as high-voltage power supplies. It also houses a filter and calibration wheel assembly for on-orbit calibration, as well as a collimator for reduction of x-ray background. At the base of the collimator is a UV/ion shield used to prevent secondary emission from the GPD. Figure 2 (right) shows a photograph of a completed flight DU.

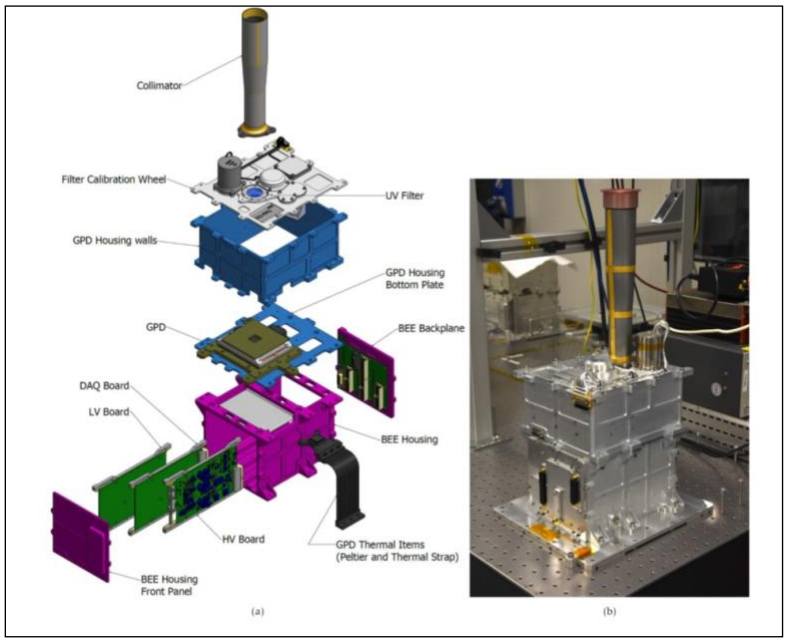

Figure 2: Expanded view of a Detector Unit (DU, left); photograph of a completed flight unit (right).

1.1.2 DU Performance

1.1.2.1 Quantum Efficiency

The quantum efficiency of the DU is the product of the quantum efficiency of the GPD and the X-ray transmission of the ion-UV filter. It was measured during calibration at INAF-IAPS for each DU.

The X-ray transmission of the ion-UV filter was measured for all the flight units and is in agreement with the expected value for 1.06 µm of Kapton coated with aluminum (50 nm) and carbon (5 nm).

The quantum efficiency of the GPD depends substantially on the DME pressure and depth, as well as the thickness of the Beryllium window. The absorption gap is measured with high precision, as is the initial gas-fill pressure, but the fill-gas pressure has been found to change with time and so has been carefully modeled to predict the pressure at launch. The resulting DU quantum efficiency reached at launch is shown in Table 2, below.

Table 2: DU quantum efficiency at launch date

DU FM#	Energy (keV)	Quantum Efficiency at Launch (%)
DU1	2.697	13.7
	6.400	1.77
DU2	2.697	13.4
	6.400	1.72
DU3	2.697	13.5
	6.400	1.74

Each DU also has an attenuating (gray) filter as part of its filter/calibration set. The X-ray transmission of these filters have been measured at different energies and are in agreement with the theoretical value expected for the 76-µm Kapton foil. Measured transmission results at two energies are given in Table 3.

Table 3: Gray filter X-ray transmission.

DU FM#	Energy (keV)	Transmission (%)
DU1	2.697	17.2 +/- 0.2

	6.400	87.7 +/- 0.5
DU2	2.697	18.1 +/- 0.2
	6.400	88.4 +/- 0.6
DU3	2.697	17.0 +/- 0.2
	6.400	88.0 +/- 0.8

1.1.2.2 Energy Resolution

Flat-field data obtained with the polarized sources were used to measure the energy resolution of each DU. This was done as the use of Bragg crystals in these sources renders the emission highly monochromatic. Spectral data were taken in 100 spots of 500-μm radius from the flat field. The energy resolution was then calculated by fitting with a Gaussian the gain-corrected energy spectrum and dividing the measured FWHM by its peak. The energy resolution as a function of energy for the three flight DUs is shown in Figure 3.

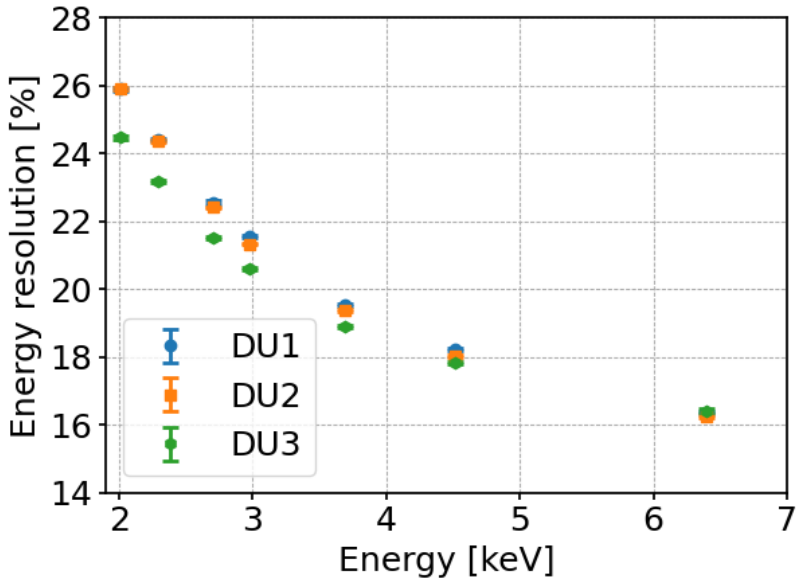

Figure 3: Energy resolution as a function of energy for the three flight DUs.

1.1.2.3 Spatial Resolution

During ground calibrations the intrinsic spatial resolution has been estimated by measuring the Half Power Diameter using a beam on-axis with diameter less than 39 micrometers (measured by a CCD test detector). Measurements have been performed for both polarized and unpolarized sources and in different points across the sensitive area of the detectors. Details of these

measurements are given in a dedicated paper in preparation (Di Marco A. et al. *Measurement of the spatial resolution of the IXPE Detector Units* '. Table 9 shows the mean results taken for the 3 flight detector units.

Table 4: Mean spatial resolution of IXPE flight DUs as a function of energy.

Energy (keV)	HPD (µm)
2.70	**116.28 +/- 0.09**
6.40	**123.5 +/- 0.4**

1.1.2.4 Modulation Factor

The modulation factor was measured at different energies and polarization angles. This provides a check- that the spurious modulation (section 1.2.5) was properly subtracted. A change of the modulation factor with polarization position angle would be expected in the presence of spurious effects, which mimic the presence of a secondary, albeit small, polarization component, and so these must be carefully removed. The net results from these measurements show that the modulation factor of the IXPE flight detectors is uniform over the detector sensitive surface and it is not dependent on polarization angle, providing evidence for correct spurious modulation removal. Calibration data have been analyzed subtracting spurious modulation using a specially-derived algorithm[4] coupled with an optimum weighting approach[5]. From these data it is possible, taking into account the GPD secular pressure variation, section 1.2.XX, to estimate the modulation

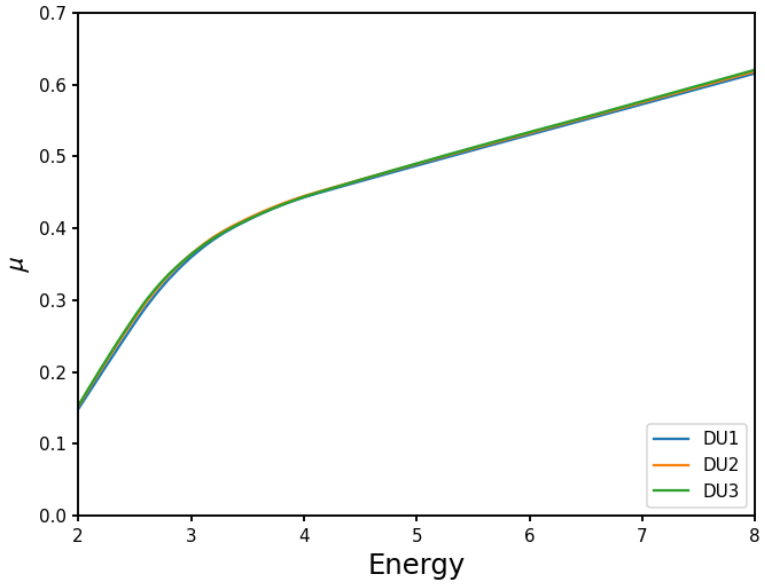

factor as a function for the time of launch, as shown in Figure 4.

Figure 4: Modulation factor as function of energy for the IXPE flight DUs estimated at time of launch

1.1.2.5 Spurious Modulation

The response of an ideal polarimeter to unpolarized radiation is statistically flat. However, IXPE focal plane detectors show, especially at low energy, a nearly-$\cos^2$ modulation which indicates the presence of a low-level spurious signal. Although the root causes of such spurious polarization have been thoroughly investigated[3] the effect is hard to model and therefore was calibrated in detail. The response of each DU was measured at six energies with a flat illumination over the entire field of view, and with higher statistics in its center where the brightest sources will be observed[6].

The spurious modulation amplitude expressed by Stokes parameters is shown in 5. In the plot, the contributions from the three IXPE DUs are summed accounting for the clocking at 120° and normalized by the corresponding modulation factor. Spurious modulation has been verified to be constant with temperature and rate using GPD prototypes constructed during IXPE development. A small time dependence has been observed, because of the variation with time of the GPD internal pressure. Such a variation, calculated for the pressure change from the calibration to the launch, is compliant with the requirement on the knowledge of spurious modulation, which is 0.3%[6].

Spurious polarization will be removed event-by-event with an algorithm developed for this purpose[7], allowing the end-user to treat data essentially as those obtained from an ideal polarimeter.

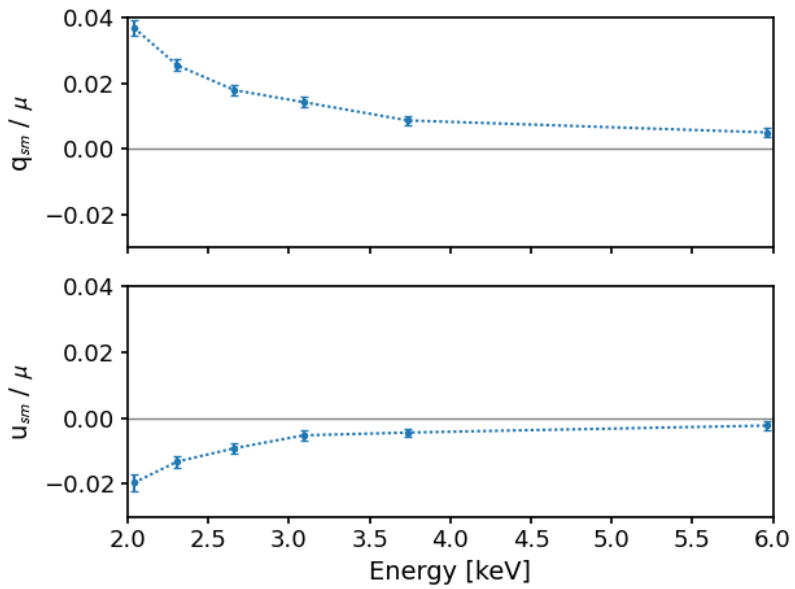

Figure *5*: Stokes parameters of spurious polarization as a function of energy of the IXPE detectors. The effect is removed during the on-ground data processing.

1.1.2.6 Rate-Dependent Gain Variations

The fine pitch of the IXPE GEMs makes them susceptible to rate-dependent gain variations due to temporary charge build-up. When the detector is irradiated, part of the charge from the avalanche can be temporarily deposited onto the dielectric substrate in the GEM holes, affecting the configuration of the electric field, and causing local (and reversible) changes in the gas gain. Since the charge trapping is not permanent, a competing discharging process is continuously at play, causing the gain to drift toward the initial value when the input energy flux is low enough.

Although this effect was largely mitigated by a dedicated fine tuning of the production process in the development stage of the mission, it is still present at a level that needs to be corrected for an accurate estimate of the energy and, since the modulation factor is energy-dependent, to correctly infer the source polarization from the measured modulation. For a typical X-ray celestial source the effect will be of the order of a few %, on timescales of several hours to a day. For very bright sources we anticipate gain variations up to 10% on much shorter timescales.

To this end, we have developed a complete phenomenological model that allows us to measure and correct such gain variations dynamically, based on the energy flux measured by the GPD as a function of time and position across the active surface. (We emphasize that all the necessary information is included in the science data that are collected during normal observations, and that the onboard calibration sources can be used to ensure that there are no systematic drifts over long observations). More details are provided in the referenced publication[3].

1.1.2.7 Long-Term Fill-Gas-Pressure Variation

Through the development of the IXPE instrument it was realized that the internal gas pressure was undergoing a long-term decrease, over timescales of months, levelling out to an overall deficit of about 150 mbar (to be compared with the nominal 800 mbar at filling time). This observation, initially hinted by a slow increase of the gas gain, has since been confirmed by several indirect evidence (including the evolution of the quantum efficiency and the average track length at a given energy), as well as direct metrological measurements of the vertical displacement of the thin Be window.

The effect has been systematically monitored using a dozen (nominally identical) detectors, with test data amounting to more than 30 GPD-years equivalent of operation. Monitoring of the energy resolution has shown no change with time, clearly indicating that no leaks are involved (and in fact the detectors are filled to less than 1 bar, so a leak would increase pressure).The cause is most likely connected to adsorption phenomena within the cell itself. The pressure decrease is unambiguously saturating with time, and in fact for the three detectors installed on IXPE are all already within a few % of the expected asymptotic value. The current rate of change, typically of the order of a 1--10 mbar per year, can be taken as a generous upper limit to the additional variations that we might expect on orbit. Onboard calibration sources will allow monitoring of the

detector evolution continuously during the mission, through the measurement of the counting rate and the average track length.

Calibration data and simulations indicate that the impact of this pressure variation on the polarimetric sensitivity is mild. While the detector quantum efficiency scales linearly with the pressure, causing a net loss of effective area, the modulation factor increases as the pressure decreases, owing to fact that the tracks become more elongated. The net effect of these two competing processes is that the relative loss of sensitivity, expressed as the broadband minimum detectable polarization for a typical source spectrum, is less than 2% when going from the nominal 800 mbar to the actual 650 mbar.

1.1.2.8 Background

The expected IXPE detector background has been modeled, taking into account the whole spacecraft and detailing the detector geometries[8]. This assessment considers all the major components of background such as the Cosmic X-ray background, albedo Gamma, and albedo neutrons, primary electron, positron, protons and alpha, secondary electron, positron and neutron. The expected counting rate from this assessment, without any background rejection, is 4.7×10^{-2} c/s/cm^2/DU over 2-8 keV, and with rejection the net rate is 1.16×10^{-3} c/s/cm^2/DU. The major contribution of un-rejected background are delta-rays from electron and positrons which are undistinguishable from source photo-electron tracks.

This level of background, approximately equal to 2 µCrab, is obviously negligible for any point sources (polarimetry is in fact photon starved and typically possible only with the brighter sources for each class). It is also negligible for most extended sources which have high surface brightness. Only 1 weak extended source, molecular clouds near the Galactic Center, may have fluxes comparable to the background. However, the slight (few %) loss of polarization sensitivity caused by this will not be of concern as the expected level of polarization for this source is very high.

1.1.3 Filter/Calibration Wheel

To enable in-flight calibration monitoring, each DU is equipped with a filter and calibration wheel assembly[9] (Figure 6). These assemblies contain various radioactive sources that can be rotated in front of the GPD to provide for monitoring gain, energy resolution, spurious modulation and modulation factor (the sensitivity to polarization for a 100% polarized source) during the mission. The calibration sources will be used in those parts of the orbit when the x-ray source under study is eclipsed by the earth, calibrating one detector at a time.

The calibration sources are all based on ^{55}Fe isotopes which have a K_α line at 5.9 keV and a K_β line at 6.5 keV. Cal source A produces polarized x rays at 3 keV (via a silver target, Si $L\alpha = 3$ keV) and at 5.9 keV, through 45° Bragg reflection off a graphite mosaic crystal. Cal sources C and D are unpolarized 5.9 keV and 6.5 keV x rays in a spot (~ 3mm) and flood (~ 15 x 15 mm) configuration respectively. Cal source D utilizes a silicon target in front of the ^{55}Fe to produce a broad beam at 1.7 keV (Si K_α). Expected count rates at the time of launch are given in Table 5, averaged over the 3 flight detectors.

In addition to the calibration sources the wheel also contains an open position, a closed position and an attenuator position consisting of a 75-µm-thick kapton foil coated with 100 nm of aluminum on each side. The first of these is for normal operations, the second for internal background measurements and the third is for observing very bright sources which would otherwise exceed the throughput of the system

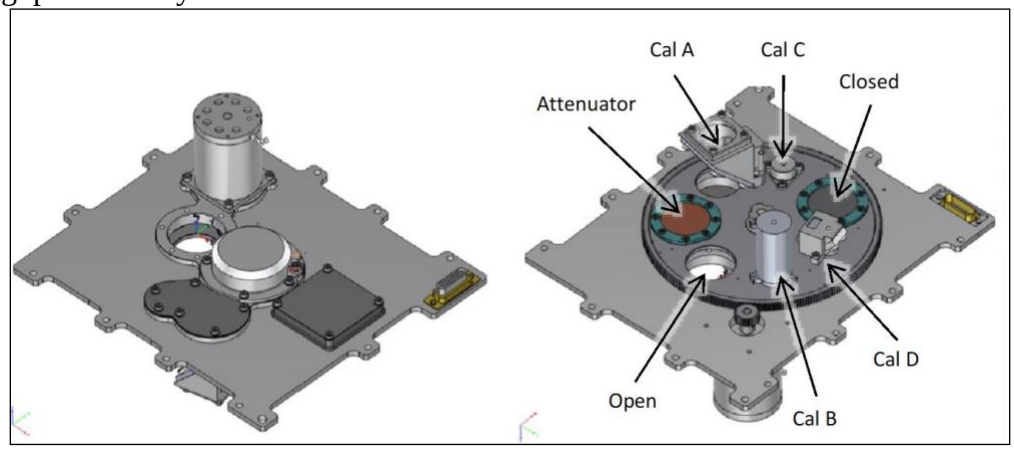

Figure 6: Filter and calibration wheel assembly (left: top view (+z); right: bottom view (-z))

Table 2: Expected count rates from on-board sources at launch

Cal Source	Count / Sec
A (5.9 keV)	33
A (3.0 keV)	2.5
B (5.9 + 6.5 keV)	62
C (5.9 + 6.5 keV)	119
D (1.7 keV)	78

1.2 Detectors Service Unit (DSU)

The principal task of the DSU is to format the DU data in a way suitable for storage in the spacecraft memory (5 GByte) and S-band downloading. The DSU also controls the filter and calibration wheels, manages the different operational modes of the DUs and supplies the necessary low-voltages.

.

Specifically, the DSU provides the following functions for the operation and autonomy of the IXPE instrument:

(1) Power supply generation (secondary power to supply the DU's sub-units).

(2) Telemetry management (data acquisition, formatting, and transmission to the S/C).

(3) Command management (reception, verification, generation, scheduling, distribution, and execution). (4) Time management (synchronization of the three DUs, GPS pulse per-second distribution, and time tagging.
(5) Filter and calibration wheel management.
(6) Science data management (retrieving, isolated pixels removal, formatting, and transmission to the spacecraft integrated avionics unit).
(7) Payload mode control.
(8) GPD temperature control.
(9) Fault detection isolation and recovery (FDIR) management.

The DSU consists of two boards with cold redundancy and one backplane for internal DSU signal routing. The boards are the single board computer and the power and service board. IXPE uses a centralized solid-state memory bank within the spacecarft for data storage and transmission. The memory onboard the DSU is used only to store the boot boot software and support the internal operations. The DSU received power from the spacecarft on two (one nominal and one redundant) unregulated power lines on separate connectors. The nominal voltage of the power lines is 28 V. Minimum and maximum values of input power provided by S/C are, respectively, 26 V and 34 V.

2 INSTRUMENT OPERATION

2.1 Modes of operation

The instrument modes of operation are managed by the DSU and are selected either via tele-command or by activating autonomously an on-board procedure set by an alarm condition which puts the instrument in a safe mode.

The modes of operation are as follows (see also Figure 7):
1. Boot, is a transitional start-up mode which occurs at power on. Boot software, runs from the programmable read-only memory (PROM) in order to perform all the checks and the initialization of the instrument. In the nominal case, the application software completes the initialization sequence by placing the instrument in standby mode (see below). The boot phase lasts around 60 s.
2. Maintenance. This mode is reserved to support the on-orbit maintenance program.
3. Stand-by. Nominally, at the end of the boot phase, the DSU transitions into stand-by mode to start the instrument monitoring and control. The stand-by mode supports: starting and handling of the thermal regulation; powering on and off the instrument systems; processing of the incoming tele-commands; and the generation of the related outgoing telemetry. Finally, it configures the detector units and the science data processing.
4. Observation. From the point of view of the DSU, all instrument calibration and scientific modes are managed into a unique observation mode that is configured while in stand-by mode. The observation mode supports the handling of thermal regulation, the handling of the time-of-day message, the collection of the housekeeping, and the generation of the scientific data.

5. South Atlantic Anomaly (SAA). This mode is used when the satellite crosses the South Atlantic Anomaly which happens once per orbit. In this mode, the high voltage (HV) is ramped down below the voltage voltage necessary for gas multiplication and the science data generation is disabled, while housekeeping data are generated and collected as usual.
6. Safe. This mode is used before switching off the instrument or performing an SW reboot and managing fault detection conditions. This mode preserves DU and HV status (i.e., no HV ramp down or switching off) when entered by telecommand. If entered by a fault condition, the HVs are ramped off, the DUs switched off, and the Filter and Calibration Wheels (FCW) rotation is set to closed as part of the recovery action. In this operation mode, the instrument generates and collects housekeeping only. It is possible to perform a reboot of the application software only during the safe mode.
7. Reboot (transitional mode). At the DSU switch-on, after the boot activities, the application software is loaded into SRAM and executed it checks the position of the FCWs and the status of the detector units and high-voltage boards. If the FCWs are closed and the high voltages are off, the software moves to standby mode. If the FCWs are not closed or if the HVBs are ON, the application software moves the FCWs to the closed position, performs the ramp-off procedure of any high voltages greater than zero, switches off the DUs, and moves the operative mode to safe.

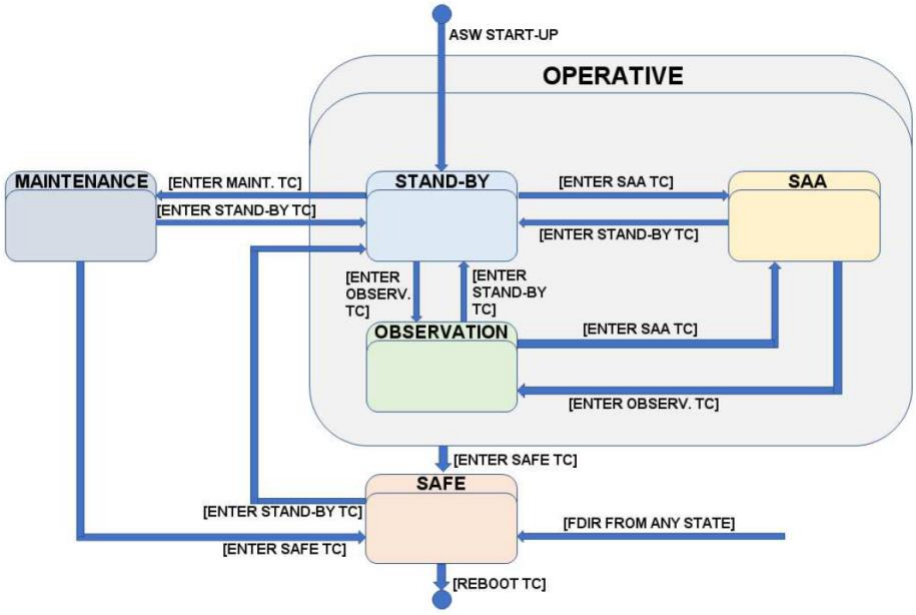

Figure 7: IXPE Instrument modes of operation

2.2 Dead time / rate capability

The dead time per event Td depends on the specifics of the readout sequence and can in general be factored into two different terms one constant and one proportional to the number of pixels $n$pix in the region of interest: $Td = d + m\ n\text{pix}$. The two coefficients depend on the particular readout settings of the back-end electronics: roughly speaking, m is mainly determined by the clock period of the serial readout while d relates to the timing constraints imposed by the ASIC for a correct

readout, and particularly the fixed delay ($\geq 400\mu s$) needed between two successive readouts. Both figures further depend on the number of additional event readouts used for the pedestal subtraction. In the nominal data-taking configuration $d \sim 750\ \mu$ s and $m \sim 600$ ns per pixel, yielding an average dead time per event slightly in excess of 1 ms for a typical ROI of 500 pixels. For one of the brightest sources planned, the Crab Nebula, this gives about 9% deadtime.

2.3 Hot pixel masking

Each DU has a specific list of noisy pixels evaluated at various times during GPD acceptance tests, DU AIV/T, DU Calibration and Instrument end-to-end tests. This list is used to mask of the noisy pixels to avoid fake triggers which could impact the data rate. The list can be evaluated and updated on board at any time if new noisy pixels appear. These can be detected on the ground with specific algorithms that analyze nominal acquisitions, both from celestial sources or calibration sources. If a pixel is masked its signal does not contribute to the trigger within its mini-cluster. It is worth noticing that since the trigger is formed by groups of 4 pixels, masking only one or two of the same mini-cluster has a small effect on the trigger efficiency if the threshold is reasonably low.

The GPD is typically operated at an effective trigger threshold of ~1000 electrons, which masks off just a handful of pixels (fewer than 1 in 10,000) and gives a noise-trigger rate of $\ll 1$ c/s. Masking the pixels involves an acquisition of just electronic noise or an acquisition with calibration sources, recording the count rate rate of each pixel, and select those with >> 1 c/s. A mask is then uploaded with the coordinates of the noisy pixels recorded and checked through housekeeping.

2.4 Timing

The GPD provides, for each processed event, a trigger output which is used to time tag each event with 1 μs resolution and 1-2 us accuracy, based on the pulse-per-second from the GPS and the instrument's 1-MHz Oscillators. The IXPE satellite manages the GPS receiver and provides the signal to the instrument through a dedicated line. The spacecraft also provides the time of day with a frequency of 1 Hz.The TOD also contains information about the validity of the previously provided PPS and the time of the next PPS.

The DSU is equipped with a temperature-compensated 1-MHz crystal oscillator (TCXO) with an accuracy <4 ppm. The PPS and the 1 MHz clock generated by the 1 MHz local oscillator are provided to each DU.

The onboard time (OBT) management is based on a master OBT implemented in the DSU and 3 local OBTs implemented in the DUs. The master OBT and the locals OBTs are composed of (i) a 29 bit counter for the seconds (>16 yr of mission lifetime) and (ii) a 20 bit counter for the microseconds (1 μs resolution) and a register for the OBT error (error counter). At boot, the master OBT is initialized by subtracting the start mission date (stored in the DSU MRAM) from the GPS time. During nominal observation, when the GPS is valid, the second counter is incremented upon receiving the PPS and the microsecond counter is incremented by the 1 MHz local oscillator. At the arrival of the PPS, the difference of the microsecond counter with respect to 10^6 is stored in the Master OBT error counter and included in the housekeeping data packet. The local OBTs in

each DU are updated by the back end electronics in the same way, using the PPS and the DSU (TCXO) clock (see Figure 8).

If the previous PPS is not valid, as indicated by the TOD, the PPS provided by the S/C is not used. The DSU synthesizes the PPS for the DUs using the local TCXO. During this operation mode, the OBT error is set equal to zero. The non valid condition information is included in the housekeeping (HK) data. The master OBT remains in free running until the reception of the sequence of TOD reporting that the PPS is again valid. In this case the DSU re-initializes the instrument timing as it would at instrument boot.
The alignment of the local OBT with the master OBT is verified using the housekeeping telemetry (TM). The HK telemetry (TM) compares the values of the local OBTs and the master OBT every second. At the MOC/SOC, these values are monitored and in cases of discrepancy, a pre-arranged action is carried out to get the times back in sync (e.g., time reset by telecommand).

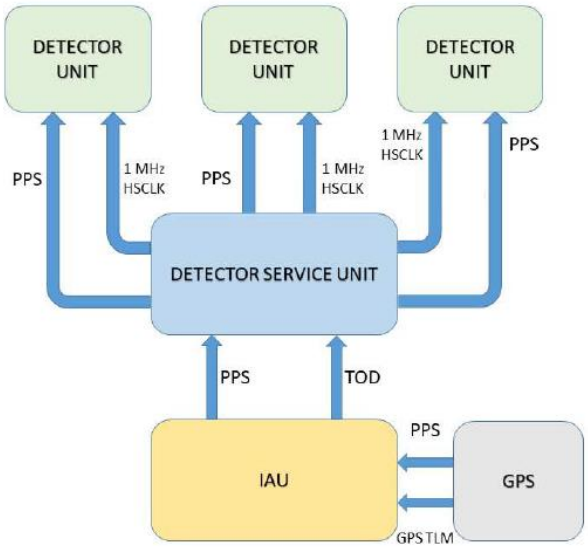

Figure 8: IXPE Instrument timing architecture.

3 REFERENCES

[1] Costa, E., Soffitta, P., Bellazzini, R., Brez, A., Lumb, N., & Spandre, G., "An efficient photoelectric X-ray polarimeter for the study of black holes and neutron stars," Nature 411, 662-665 (2001).

[2] Bellazzini, R., Spandre, G., Minuti, M., Baldini, L., Brez, A., Latronico, L., Omodei, N., Razzano, M., Massai, M. M., Pesce-Rollins, M., Sgro, C., Costa, E., Soffitta, P., Sipila, H., & Lempinen, E., "A sealed Gas Pixel Detector for X-ray astronomy," NIMPA 579, 853-858 (2007).

[3] Baldini L., Barbanera M., Bellazzini R., Bonino R., Borotto F, Brez A., Caporale C., Cardelli C., Castellano S., Ceccanti M., Citraro S., Di Lalla N., Latronico L., Lucchesi L., Magazz`u C., Magazz`u G., Maldera S., Manfreda A., Marengo M., Marrocchesi A., Mereu P., Minuti M., Mosti F., Nasimi H., Nuti A., Oppedisano C., Orsini L., Pesce-Rollins M., Pinchera M., Profeti A., Sgr`o C., Spandre G., Tardiola M., Zanetti D., Amici F., Andersson H., Attin`a, P., Bachetti M., Baumgartner W., Brienza D., Carpentiero R., Castronuovo M., Cavalli L., Cavazzuti E., Centrone M., Costa E., D'Alba E., D'Amico F., Del Monte E., Di Cosimo S., Di Marco A., Di Persio G., Donnarumma I., Evangelista,Y., Fabiani S., Ferrazzoli R., Kitaguchi T., La Monaca F., Lefevre C., Loffredo P., Lorenzi P., Mangraviti E., Matt G., Meilahti T., Morbidini A., Muleri F., Nakano T., Negri B., Nenonen S., O'Dell S. L., Perri M., Piazzolla R., Pieraccini S., Pilia M., Puccetti S., Ramsey B. D., Rankin J., Ratheesh A., Rubini A., Santoli F., Sarra P., Scalise E., Sciortino A., Soffitta P., Tamagawa T., Tennant A., Tobia A., Trois A., Uchiyama K., Vimercati M., Weisskopf M. C., Xie F., Zanetti F., Zhou Y., Design, Construction and Test of the Gas Pixel Detectors for the IXPE Mission, arXiv, arXiv:2107.05496, to be published in Astroparticle Physics, (2021).

[4] John Rankin et al., "An algorithm to calibrate and correct the response to unpolarized radiation of the X-ray polarimeter on board IXPE" submitted to Astronomical Journal (2021).

[5] Alessandro Di Marco et al., "A weighted analysis to improve the X-ray polarization sensitivity of IXPE" submitted to Astronomical Journal (2021).

[6] Muleri F. et al., 'Response of the IXPE Detector Units to unpolarized radiation' in preparation (2021).

[7] Rankin J. et al., "An algorithm to calibrate and correct the response to unpolarized radiation of the X-ray polarimeter on board IXPE" submitted to Astronomical Journal (2021).

[8] Fei Xie, F., Ferrazzoli, R., Soffitta, P., Fabiani S., Costa, E., Muleri, F., Di Marco, A. "A study of background for IXPE" Astroparticle Physics 128, (2021), 102566

[9] Ferrazzoli, R., Muleri, F., Lefevre, C., Morbidini, A., Amici, F., Brienza, D., Costa, E., Del Monte ,E., Di Marco, A., Di Persio, G., Donnarumma, I., Fabiani, S., La Monaca, F., Loffredo, P., Maiolo, L., Maita, F., Piazzolla, R., Ramsey, B., Rankin, J., Ratheesh, A., Rubini, A., Sarra, P., Soffitta, P., Tobia, A. & Xiea, F., "In-flight calibration system of imaging x-ray polarimetry explorer", J. Astron. Telesc. Instrum. Syst., Vol 6(4), (2020).